*Journal of Biomolecular NMR*, **14:** 373–376, 1999.
*KLUWER/ESCOM*



# Resonance assignments, secondary structure and $^{15}$N relaxation data of the human transcriptional coactivator hMBF1 (57-148)

Masaki Mishima[a], Jun Ozaki[a], Takahisa Ikegami[a], Yasuaki Kabe[b], Masahide Goto[b], Hitoshi Ueda[c], Susumu Hirose[c], Hiroshi Handa[b] & Masahiro Shirakawa[a,*]
[a]*Graduate School of Biological Sciences, Nara Institute of Science and Technology, 8916-5 Takayama, Ikoma, Nara 630-0101, Japan;* [b]*Department of Developmental Genetics, National Institute of Genetics, Mishima, Shizuoka-Ken 411, Japan;* [c]*Faculty of Bioscience and Biotechnology, Tokyo Institute of Technology, Midori-ku, Yokohama 226, Japan*

Received 6 February 1999; Accepted 25 June 1999

*Key words:* $^{15}$N relaxation, resonance assignment, secondary structure, transcriptional coactivator

**Abstract**

Multiprotein bridging factor 1 (MBF1) is a transcriptional coactivator that is thought to bridge between the TATA box-binding protein (TBP) and DNA binding regulatory factors, and is conserved from yeast to human. Human MBF1 (hMBF1) can bind to TBP and to the nuclear receptor Ad4BP, and is suggested to mediate Ad4BP-dependent transcriptional activation. Here we report the resonance assignments and secondary structure of hMBF1 (57–148) that contains both TBP binding and activator binding residues. $^{15}$N relaxation data were also obtained. As a result, hMBF1 (57–148) was shown to consist of flexible N-terminal residues and a C-terminal domain. The C-terminal domain contains four helices and a conserved C-terminal region.

Transcriptional coactivators play a crucial role in gene expression by communicating between regulatory factors and the basal transcription machinery. Multiprotein Bridging Factor type 1 (MBF1) is a transcriptional coactivator that bridges between the TATA box-binding protein (TBP) and DNA binding regulatory factors, and is conserved from yeast to human (Takemaru et al., 1997). By *in vitro* transcription assays, *B. mori* MBF1 was shown to recruit TBP to a promoter carrying the FTZ-F1-binding site by bridging TBP and the nuclear receptor FTZ-F1 (Li et al., 1994). Likewise, yeast MBF1 has been shown to mediate GCN4-dependent transcriptional activation by bridging the DNA-binding region of GCN4 and TBP (Takemaru et al., 1998), suggesting that MBF1 mediates transcriptional activation by recruiting TBP to promoters where the DNA-binding regulators are bound.

hMBF1 cDNA sequence was originally identified as a homologue of *B. mori* MBF1 in the databases, and subsequently the cDNA was cloned from HeLa c-DNA library (Takemaru et al., 1997; Kabe et al.,

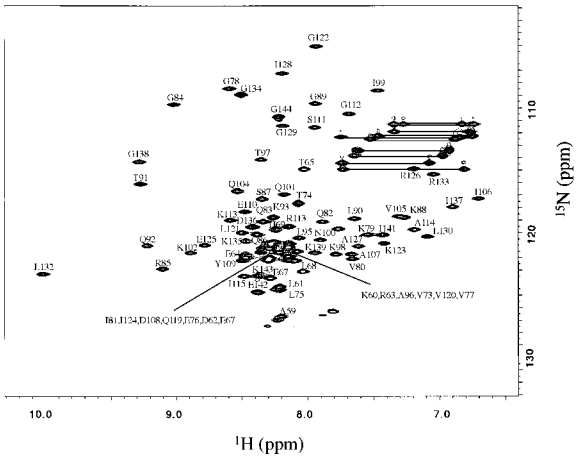


*Figure 1.* $^{1}$H-$^{15}$N HSQC spectrum of hMBF1 (57–148). Assignment of cross-peaks is shown using the one-letter code for amino acids. Pairs of peaks connected by horizontal lines represent Gln and Asn side chain $NH_2$ groups.

*To whom correspondence should be addressed.

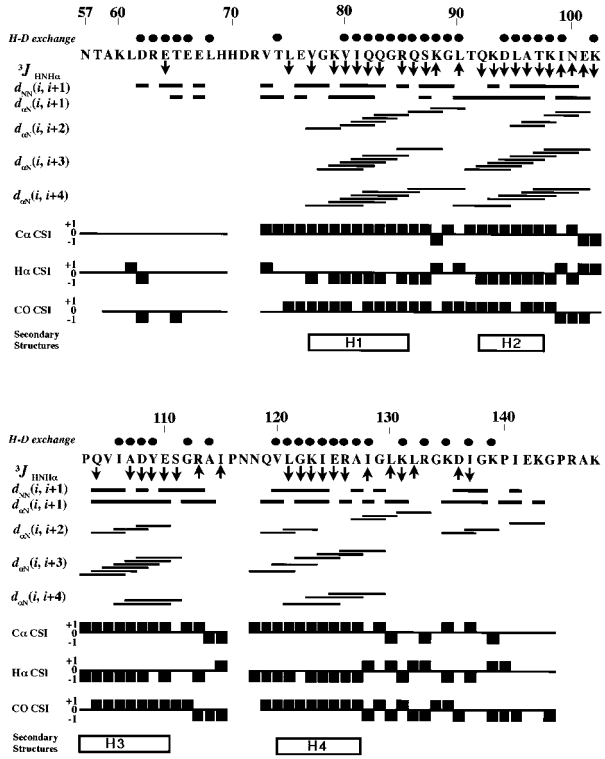


*Figure 2.* Primary sequence of hMBF1 (57–148) with a summary of short and medium range NOEs, NH exchange data, CSI data and $^3J_{HNH\alpha}$ coupling constants. Circles above the sequence indicate residues with amide protons visible in the $^{15}$N HSQC spectrum after 25 min of solvent exchange in $D_2O$ buffer at 37 °C, pH 6.5. The CSI data obtained from $^{13}C_\alpha$, $^1H_\alpha$ and $^{13}C'$ chemical shift data are represented by square bars (Wishart and Sykes, 1994). Upward and downward arrows indicate the coupling constants >8 Hz and <4 Hz, respectively.

submitted). It was found that hMBF1 interacts with the DNA-binding region of ATF-1 or Ad4BP *in vitro*, in addition to TBP (Kabe et al., submitted). Transient expression of hMBF1 in HeLa cells causes an elevated transcription of the gene carrying the binding sites of Ad4BP or ATF-1. These data suggest that hMBF1 serves as a coactivator of ATF-1 and Ad4BP. By deletion analysis, a truncated hMBF1 containing amino acids 67–148 has been shown to bind to TBP, and either of ATF-1 or Ad4BP (Kabe et al., submitted). Recently, Dragoni et al. (1998) identified EDF-1, which is identical with hMBF1, as a gene product down-regulated in human endothelial cell differentiation. Herein, we report the NMR resonance assignments and the secondary structure of hMBF1 (57–148).

hMBF1 (57-148) was expressed in *E. coli* using the pET16b vector (Novagen). For the NMR experiments a uniformly $^{15}$N or $^{15}$N/$^{13}$C-labeled protein was produced by growing *E. coli* in M9 medium containing $^{15}NH_4Cl$, without or with [U-$^{13}$C]-glucose, respectively. Cells were lysed by sonication, and the recombinant proteins were purified by SP-Sepharose (Pharmacia) and Mono-S (Pharmacia) ion-exchange and Sephacryl S-100 (Pharmacia) gel-filtration chromatographies. The homogeneity of purified hMBF1 (57-148) was estimated from SDS-polyacrylamide gel electrophoresis and Coomassie Blue staining. Three mg of pure (>95%) hMBF1 (57–148) was obtained from a 2 L culture, and it was found to be monomeric in solution by gel-filtration chromatography.

Samples for NMR measurements typically comprised 0.5–2.0 mM protein in 50 mM potassium phosphate buffer (pH 6.5), 50 mM KCl, 0.1 mM EDTA in $H_2O/^2H_2O$ (9/1). All NMR spectra were recorded at 37 °C with Bruker DMX500, DRX500 or DRX800 spectrometers. Sequential resonance assignments of backbone $^1$H, $^{15}$N and $^{13}$C atoms were obtained from 3D experiments, CBCANH, CBCA(CO)NH, HN(CA)CO, HNCO, and verified by a 3D $^{15}$N NOESY-HSQC spectrum (Cavanagh et al., 1996). The assignments are indicated in the HSQC spectrum in Figure 1. Sidechain $^1$H and $^{13}$C assignments were obtained from a series of 3D experiments, $^{15}$N

TOCSY-HSQC (Cavanagh et al., 1996), H(CCO)NH (Grzesiek et al., 1993), C(CO)NH (Grzesiek et al., 1993) and HCCH-TOCSY (Cavanagh et al., 1996). Stereospecific assignments of γ methyl groups of valines and δ methyl groups of leucines were made using a 15% fractionally $^{13}$C-labeled protein and $^{13}$C HSQC experiments (Szyperski et al., 1992).

Most of $^{1}$H, $^{15}$N, and $^{13}$C backbone and sidechain assignments have been made, except for 70–72, 116–118, 145–148. Most of the mainchain amide signals for these residues could not be observed in the $^{1}$H-$^{15}$N HSQC experiment, possibly due to local exchange broadening and/or rapid exchange of the amide protons with the solvent. The $^{1}$H, $^{13}$C and $^{15}$N chemical shifts for hMBF1 (57–148) have been deposited in the BioMagResBank (http://www.bmrb.wisc.edu) under BMRB accession number 4294.

The secondary structure of hMBF1 (57–148) is analyzed by means of chemical shift indices (CSI), sequential- and medium-range NOE patterns, the backbone vicinal coupling constants, $^{3}J_{HNH\alpha}$, and amide proton exchange rates (Figure 2). The CSI analysis using $^{13}$Cα, $^{1}$Hα, and $^{13}$C′ shifts suggests that hMBF1 (57–148) has four helical regions. There is no indication that hMBF1 (57–148) has a β-strand or a continuous extended conformation. Interproton distances were derived from 3D experiments, $^{13}$C NOESY-HSQC and $^{15}$N NOESY-HSQC, and 4D experiments, $^{13}$C/$^{15}$N edited HMQC-NOESY-HSQC and $^{13}$C/$^{13}$C edited HMQC-NOESY-HSQC (Cavanagh et al., 1996). Backbone dihedral angles were estimated from vicinal coupling constants ($^{3}J_{HNHa}$) obtained from HMQC-J experiments (Kay and Bax, 1990). The results obtained from the combined analysis of short- and medium range NOEs, the vicinal coupling constants and hydrogen exchange rates are in good agreement with those obtained by the CSI analysis, and indicate that hMBF1 (57–148) has four helical regions: H1 (77–85), H2 (92-97), H3 (103–110), H4 (120–127). Because stretches of $d_{\alpha N}(i, i+4)$ connectivities were found, it is suggested that these helical regions form mainly α-helical conformations. Although stretches of several $d_{\alpha N}(i, i+2)$ connectivities are observed in the helical regions, which are often observed for $3_{10}$-helices, the signals for them were weak in NOESY spectra and thus probably due to spin diffusion effects.

Few medium- and no long-range NOEs were observed for the N-terminal region, residues 57–75, suggesting that this region is not well structured. In order to obtain a direct measure of the protein flexibility, relaxation data of the mainchain $^{15}$N resonances were obtained. Spectra for $^{15}$N $T_1$, $T_2$, and $^{1}$H-$^{15}$N steady-state heteronuclear NOE values were acquired at 37 °C and a $^{15}$N frequency of 50.7 MHz. Enhanced-sensitivity pulse sequences were used (Farrow et al., 1994). The $T_1$ relaxation delays were 19, 64, 144, 244, 364, 524, 754, 1144, 1449, 1724 and 1999 ms and the $T_2$ relaxation delays were 14.4, 28.8, 43.2, 57.6, 72.0, 100.8, 144.0, 187.2, 244.8 and 345.6 ms. The delay between $^{15}$N 180° pulses in the CPMG sequence for the $T_2$ measurements was 900 μs. In the $^{1}$H-$^{15}$N NOE experiments, relaxation delays of 3.6 s before the $^{1}$H saturation were applied. The $^{1}$H saturation was achieved for 3.0 s with 120° $^{1}$H pulses applied every 5 ms. Peak heights of each spectrum were obtained. Each $T_1$ and $T_2$ was determined by fitting the measured intensities by a two-parameter single-exponential function using the program CURVEFIT, as described previously (Ikegami et al., 1999; Mandel et al., 1995). The uncertainties in the measured peak heights for the $T_1, T_2$ and NOE measurements were estimated by repeating the experiments [$T = 19$ ms for the $T_1$ measurements, and $T = 14.4$ ms for the $T_2$ measurements]. The uncertainties were calculated by the associated programs in the Modelfree v.4.0 package (Mandel et al., 1995). The obtained $^{15}$N $T_1$, $T_2$, and $^{1}$H-$^{15}$N steady-state heteronuclear NOE values are shown in Figure 3. Most $T_1$ and $T_2$ data for the $^{15}$N spins in the 13 N-terminal residues (57 to 69) could not be fit by the function within $\chi^2$ values smaller than the tabulated $\chi^2$ values at the 95% confidence level.

For helical regions of the protein, residues 77–85, 92–97, 103–110 and 120–127, both $T_1$ and $T_2$ values are rather uniform: they are $443 \pm 12$ ms and $138 \pm 6$ ms, respectively. Large and uniform $^{1}$H-$^{15}$N steady-state heteronuclear NOE values, $0.68 \pm 0.04$, are also observed in these regions, suggesting that the helical regions are well-structured, and tumble at the same overall rate. It is of interest that large NOE values are observed for a part near the C-terminus, residues 128–139. The sequence in this region is well conserved across MBFs from yeast to human (Takemaru et al., 1997), containing basic and hydrophobic residues, Leu 128, Lys 131, Leu 132, Arg 133 and Lys 135 which are almost identical across the MBF1 sequences. The high NOE values and the high sequence conservation suggest that this region might be part of a structured domain, although any regular secondary structure was not identified in the region. In contrast, small or negative NOE values were observed for the N- and C-terminal regions, residues 57–75 and

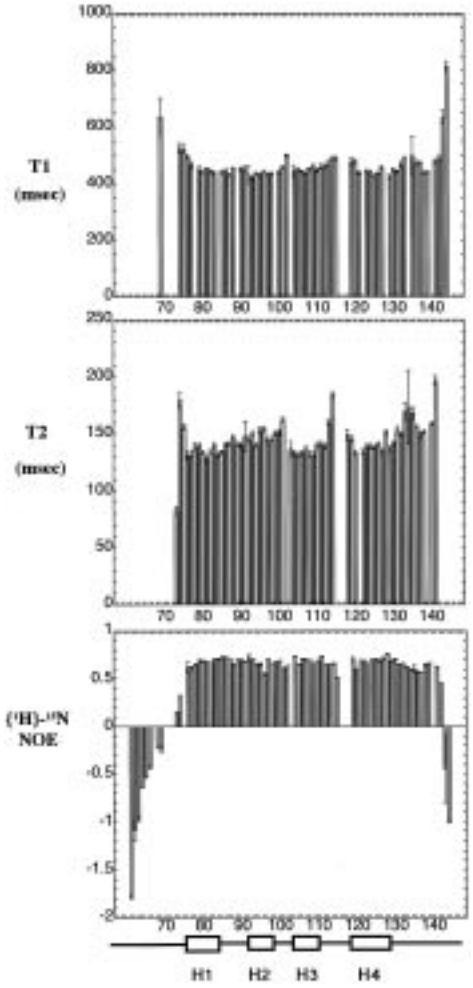


*Figure 3.* Plots of amide $^{15}N$ $T_1$, $T_2$, and $\{^1H\}$-$^{15}N$ steady-state heteronuclear NOE against residue numbers. The data were measured at a $^{15}N$ frequency of 50.7 MHz. The error bars indicate the $\pm$SD ($1\delta$) values of the uncertainties of the data. The secondary structures are indicated at the bottom.

142–148 (except for missing signals), indicating that these N- and C-terminal sequences are highly mobile in solution relative to the overall tumbling rate of the molecule.

The presence of the N-terminal flexible part and the C-terminal structured domain may be a common feature of MBF1s. Based on a limited digestion of *B. mori* MBF1 and NMR spectra, it was recently shown that the C-terminal 80 residues of *B. mori* MBF1 form a well structured domain (Ozaki et al., in press), which is capable of binding to TBP (Takemaru et al., 1997). This C-terminal domain of *B. mori* MBF1 also consists of four helical regions and the C-terminal residues as hMBF1 (57–148) does (Ozaki et al., in press), suggesting that the structural feature of the C-terminal domains is conserved between *B. mori* and human MBF1s. Takemaru et al. (1998) showed that substitution of alanine for aspartic acid at position 112 of yeast MBF1 resulted in a large reduction of its binding to TBP *in vitro* and a consequent loss of function *in vitro*: yeast cells harboring this mutant were sensitive to aminotriazole, an inhibitor of the *HIS3* gene product. The acidic residue is conserved at this position across all the aligned MBF1 sequence (Takemaru et al., 1997). The corresponding residue in hMBF1 is Asp 108, and is located in the helix H3, suggesting that H3 serves as a binding site with TBP. To date, little is known about structures of coactivators that bind to TBP. Our data, as well as data about *B. mori* MBF1, now provide the basis for the interaction of the coactivators with TBP and a framework for the structural analysis of transcription activations.

## Acknowledgements

This work was supported by grants to M.S. and T.I. from the Ministry of Education, Science, and Culture of Japan.

## References

Cavanagh, J., Fairbrother, W.J., Palmer III, A.G. and Skelton, N.J. (1996) *Protein NMR Spectroscopy*, Academic Press, San Diego, CA.

Dragoni, I., Mariotti, M., Consalez, G.G., Soria, M.R. and Maier, J.A. (1998) *J. Biol. Chem.*, **273**, 31119–31124.

Farrow, A.N., Muhandiram, R., Singer, A.U., Pascal, S.M., Kay, C.M., Gish, G., Shoelson, S.E., Pawson, T., Forman-Kay, J.D. and Kay, L.E. (1994) *Biochemistry*, **33**, 5984–6003.

Grzesiek, S., Anglister, J. and Bax, A. (1993) *J. Magn. Reson.*, **B101**, 114–119.

Ikegami, T., Kuraoka, I., Saijo, M., Kodo, N., Kyogoku, Y., Morikawa, K., Tanaka, K. and Shirakawa, M. (1999) *J. Biochem.*, **125**, 495–506.

Kabe, Y., Goto, M., Shima, D., Wada, T., Morohashi, K., Shirakawa, M., Hirose, S. and Handa, H., submitted.

Kay, L.E. and Bax, A. (1990) *J. Magn. Reson.*, **86**, 110–126.

Li, F.-Q., Ueda, H. and Hirose, S. (1994) *Mol. Cell. Biol.*, **14**, 3013–3021.

Mandel, A.M., Akke, M. and Palmer III, A.G. (1995) *J. Mol. Biol.*, **246**, 144–163.

Ozaki, J., Ikegami, T., Takemaru, K., Ueda, H., Hirose, S., Kabe, Y., Handa, H. and Shirakawa, M., in press.

Szyperski, T., Neri, D., Leiting, B., Otting, G. and Wüthrich, K. (1992) *J. Biomol. NMR*, **2**, 323–334.

Takemaru, K., Li, F.-Q., Ueda, H. and Hirose, S. (1997) *Proc. Natl. Acad. Sci. USA*, **94**, 7251–7256.

Takemaru, K., Harashima, S., Ueda, H. and Hirose, S. (1998) *Mol. Cell. Biol.*, **18**, 4971–4976.

Wishart, D.S. and Sykes, B.D. (1994) *J. Biomol. NMR*, **4**, 171–180.